Title

Design principles of a conditional futile cycle exploited for regulation

Journal

Molecular Omics, 11(7)

ISSN

2515-4184

Authors

Tolla, Dean A
Kiley, Patricia J
Lomnitz, Jason G
et al.

Publication Date

2015-07-01

DOI

10.1039/c5mb00055f

Peer reviewed

HHS Public Access

Author manuscript

Mol Biosyst. Author manuscript; available in PMC 2016 July 01.

Published in final edited form as:

Mol Biosyst. 2015 July ; 11(7): 1841–1849. doi:10.1039/c5mb00055f.

Design Principles of a Conditional Futile Cycle Exploited for Regulation

Dean A. Tolla[a], **Patricia J. Kiley**[c], **Jason G. Lomnitz**[a], and **Michael A. Savageau**[a,b,*]

[a]Biomedical Engineering Department University of California, One Shields Ave, Davis, CA 95616 USA

[b]Microbiology Graduate Group, University of California, One Shields Ave, Davis, CA 95616 USA

[c]Department of Biomolecular Chemistry, University of Wisconsin, 1300 University Avenue, Madison, WI 53706

Abstract

In this report, we characterize the design principles of futile cycling in providing rapid adaptation by regulatory proteins that act as environmental sensors. In contrast to the energetically wasteful futile cycles that are avoided in metabolic pathways, here we describe a conditional futile cycle exploited for a regulatory benefit. The FNR (fumarate and nitrate reduction) cycle in *Escherichia coli* operates under two regimes – a strictly futile cycle in the presence of O_2 and as a pathway under anoxic conditions. The computational results presented here use FNR as a model system and provide evidence that cycling of this transcription factor and its labile sensory cofactor between active and inactive states affords rapid signaling and adaptation. We modify a previously developed mechanistic model to examine a family of FNR models each with different cycling speeds but mathematically constrained to be otherwise equivalent, and we identify a trade-off between energy expenditure and response time that can be can be tuned by evolution to optimize cycling rate of the FNR system for a particular ecological context. Simulations mimicking experiments with proposed double mutant strains offer suggestions for experimentally testing our predictions and identifying potential fitness effects. Our approach provides a computational framework for analyzing other conditional futile cycles, which when placed in their larger biological context may be found to confer advantages to the organism.

Keywords

futile cycling; biochemical systems theory; design principles; FNR; oxygen sensing

Introduction

Cycles are a recurrent theme of molecular biology and occur throughout the biological world at both the macro and micro scale. At the metabolic level there are numerous pathways that have the potential to operate as cycles. The term ‘futile’ cycle has often been used to describe cycles that were poorly understood; the term is still applied in a loose fashion even

*Corresponding Author: masavageau@ucdavis.edu, Tel. +1 530 754 7350, Fax +1 530 754 5739.

when the cycle clearly performs a useful function. For our purposes, we will use the term futile cycle in a strict sense to refer to a system in which a molecule undergoes a series of two or more reactions before returning to its original state with no overall effect other than the dissipation of energy. We expect that such cycles would be very rare, and note that to obtain conclusive proof that a cycle serves no function is an extremely difficult task.

In every well-studied case, a cycle that may have appeared futile initially has eventually been understood to serve an important function. This includes the classic example of fructose-6-phosphate phosphorylation-dephosphorylation, which is still commonly referred to as a futile cycle despite fructose-1,6-bisphosphate having been established as an important allosteric regulator of pyruvate kinase[1,2]. From an uninformed perspective, kinetic proofreading in protein translation would look like a system in which a charged tRNA, an elongating peptide chain, and the ribosome expend GTP only to cycle a charged tRNA in and out of the ribosomal A site[3–5]. In general, there are an enormous number of enzymes with reciprocal function capable of forming a cycle that on the surface could appear futile. This would include cycles such as uridylation-deuridylation, phosphorylation-dephosphorylation, acetylation-deacetylation, and adenylation-deadenylation. These cycles serve to regulate, power, and regenerate a staggering number of cellular mechanisms and clearly cannot be considered futile.

In contrast to the above examples, the FNR (fumarate and nitrate reduction) cycle in *Escherichia coli* operates under two regimes – a strictly futile cycle in the presence of O_2 and as a pathway under anoxic conditions [for review see[6]]. The cycling of FNR is driven by O_2[7–9], and in accordance with the strict definition of a futile cycle, deletion of the *fnr* gene does not affect the growth of cells under aerobic conditions[10]. However, under anaerobic conditions FNR is required for adapting cells to the anoxic environment as it is the master regulator of the decision to induce anaerobic growth[11–13]. Thus, the FNR cycle is a *conditional* futile cycle, and in this larger context, it can be said that such a system is not truly futile.

The mechanisms of FNR cycling have been well studied. Initially, O_2 causes conversion of the $[4Fe\text{-}4S]^{2+}$ cluster to a $[2Fe\text{-}2S]^{2+}$ form, which destabilizes dimeric [4Fe-4S]-FNR[6–8,14–16]. A further reaction with O_2^- causes the monomeric [2Fe-2S]-FNR to lose its Fe-S cluster altogether, which returns it to the apoprotein state[15]. The inactive monomer is subject to active decay by ClpXP, whereas dimeric FNR is protected from proteolysis[17]. The inactive monomer is also predicted to be resynthesized into [4Fe-4S]-FNR via the Isc iron-sulfur cluster assembly pathway, which catalyzes FNR Fe-S cluster biogenesis under both aerobic and anaerobic conditions[7,9,15,16]. Fig. 1 summarizes the essential features of the FNR regulatory network.

The cycle of synthesis and degradation of [4Fe-4S]-FNR under aerobic conditions limits FNR dependent transcriptional regulation to mainly anaerobic conditions. As mentioned above, mutants lacking this regulator have no aerobic growth phenotype despite the fact that synthesis of the [4Fe-4S] cluster consumes valuable cellular resources such as reduced iron and the amino acid cysteine, the sulfur donor. Although the forms of iron released after cluster destruction in cells has not been completely resolved, it likely accumulates in an

oxidized state, which would require energy to return iron to the reduced form and energy would also be required to provide sufficient cysteine for new cluster synthesis. The operation of the FNR circuit as a pathway under anaerobic conditions and as a futile cycle under aerobic conditions raises the question of what advantage offered by conditional futile cycling compensates for the seemingly wasteful expense of energy and other resources. Perhaps such cycles facilitate a rapid response to environmental signals; in accordance with this hypothesis, *E. coli* might be expected to benefit from the ability to switch rapidly between aerobiosis and anaerobiosis.

Our previous work produced a robust model of the FNR system that integrated existing experimental data into a cohesive system, made predictions of mutant behavior that were validated by experimental data, predicted the dynamics of the aerobic-to-anaerobic transition, and provided estimates of active FNR *in vivo*[18,19]. Here, we expand on the previous work with a more detailed analysis of the FNR system in order to understand how cycling rate impacts the design of a gene circuit, particularly in conferring a rapid response to environmental signals. Unlike the earlier work, which only dealt with the natural cycling rate, we now consider a family of related FNR models that differ in their cycling rate but are otherwise constrained in a well-controlled fashion to be identical in other respects. This allows us to determine whether or not there is an optimal cycling rate in a particular ecological context, to estimate additional rate constants based on experimental evidence, and to test the feasibility of a method for assessing the dynamics of FNR activation and inactivation. We find a trade-off between energy expenditure and response time that can be can be tuned by selection to optimize cycling rate of the FNR system and provide a rapid response to changes in the O_2 content of the environment.

Results and Discussion

Many molecular systems operate or have the potential to operate as cyclic systems. As these systems have become better understood they typically cease to appear futile and have become associated with a spectrum of discovered functions. Glycolysis and gluconeogenesis are one example in which regulation prevents futile cycling between glucose and pyruvate, which would consume ATP without a useful function[20]. To understand how the seemingly wasteful cycling of the FNR protein provides a benefit to the O_2 sensing abilities of the cell, we identified and systematically analyzed several system attributes relevant to cycling. The following is an overview of the results that will be provided in this section. First, we briefly describe our previously developed model in sufficient detail to allow an appreciation for the changes being made to examine alternative cycling rates. Second, we describe a method to experimentally validate the dynamics predicted in this report. Third, we mathematically compare a family of modified FNR systems each with a different cycling speed that are otherwise equivalent.

Model of the FNR System

Our previous efforts led to the formulation of a robust model of FNR regulation. We outline the central features of the model in reference to the simplified diagram in Fig. 2 [for further detail see[18,19]]. The inactive monomeric forms of FNR were aggregated into a single

variable (X_2) to simplify the model without significant loss of information, as both apoFNR and 2Fe-FNR are inactive FNR monomers that share similar protein degradation kinetics[17]. The model is composed of sums of power-law expressions, Hill functions, and a hyperbolic rate law for repression.

$$\frac{dX_1}{dt}=\frac{\alpha_{1,\max K_1}}{X_3+K_1}-\frac{(\beta_{1,\min}K_2^n+\beta_{1,\max}X_6^n)X_1}{X_6^n+K_2^n} \quad (1)$$

$$\frac{dX_2}{dt}=\alpha_{21}X_1+2\alpha_{22}X_3X_6-\frac{(\beta_{21,\min}K_2^n+\beta_{21,\max}X_6^n)X_2X_4}{X_6^n+K_2^n}-2\beta_{22}X_2^2X_5 \quad (2)$$

$$\frac{dX_3}{dt}=\beta_{22}X_2^2X_5-\alpha_{22}X_3X_6-\frac{(\beta_{3,\min}K_2^n+\beta_{3,\max}X_6^n)X_3}{X_6^n+K_2^n} \quad (3)$$

Rate constants marked with max or min reflect the fact that this model bridges two distinct environments, an aerobic environment in which O_2 is abundant ($X_6 > K_2$) and an anaerobic environment in which O_2 is limiting or absent ($X_6 < K_2$). Maximal rate constants correspond to the aerobic environment in which cells grow faster, and minimal rate constants correspond to the anaerobic environment in which cells grow slower. Equation (1) describes the mRNA pool (X_1) for which the rate of synthesis involves a hyperbolic rate law under repression-mediated control by the active 4Fe-FNR dimer (X_3). The decay kinetics of the *fnr* mRNA are sensitive to the cellular environment and follow their maximum decay rate under aerobic conditions ($X_6 > K_2$) or their minimum decay rate under anaerobic conditions ($X_6 < K_2$). Equation (2) describes the apoFNR and 2Fe-FNR pool (X_2). The description includes two positive terms – the rate of apoFNR synthesis and the rate of 4Fe-FNR conversion into 2Fe-FNR – along with three negative terms – the rate of apoFNR-2Fe-FNR degradation via ClpXP (X_4) at the minimal rate, or at its maximal rate, and the dimerization rate (X_5) of apoFNR-2Fe-FNR into 4Fe-FNR. Equation (3) describes the 4Fe-FNR pool (X_3) whose rate of change depends on influx from the apoFNR-2Fe-FNR pool, O_2 (X_6) dependent efflux back to the apoFNR-2Fe-FNR pool, and loss due to dilution resulting from cell growth either at the maximal or minimal rate. The parameter values in our model have been determined from experimental data for *E. coli* under laboratory conditions. It should be noted that although these conditions are intended to reflect the dominant features of the organism's natural environment, many of the actual conditions in the major environments of *E. coli* are complex and largely unknown[21].

Inferring Dynamics of Active FNR by Means of a Reporter Bioassay

To better understand the importance of futile cycling and its effects on the response time of the FNR system, we propose a reporter bioassay for the active form of FNR and simulate the expected dynamics. As the reference to which these simulated dynamics will be compared, we summarize the salient features of the predicted response from our previous model.

Transitions from aerobic to anaerobic growth states correspond to an interruption of the FNR cycle (by loss of O_2), whereas the anaerobic-to-aerobic shift corresponds to the restoration of the cycle (by return of O_2). The complete dynamic response (Fig. 3, solid lines) following a shift in O_2 conditions reveals two key temporal characteristics: The peak time, which is defined as the time at which the concentration of active FNR reaches its maximum or minimum, and the settling time, which is defined as the time at which the concentration of active FNR reaches and remains within ±5% of its final steady state. The overshoot (see double arrows in Fig. 3) and subsequent settling of active FNR results from the combination of three factors: interruption (loss of O_2) or restoration (return of O_2) of the cycle, slow loss of either active or inactive FNR relative to the cycling rate, and negative feedback of active FNR on the transcription of *fnr*. These three factors are discussed in detail below and in the Supplemental Information.

In the case of the aerobic-to-anaerobic transition, our predicted dynamics show that the sudden interruption of the futile cycle produces an extremely rapid rise in active FNR levels, which is reflected in the initial dynamics observed in the first three minutes in Fig. 3A (solid lines). Once the majority of FNR is in the active form, the primary mode of loss is dilution due to cell growth. Because the dilution process is significantly slower than the initial buildup that results from interrupting the cycle, the time course predicted for settling to the new *anaerobic* steady state is quite slow. The influence of negative feedback in the case of the FNR system (Fig. 2) prevents the system from expanding the total FNR pool. Indeed, it has been shown experimentally[22] and in our model[18] that repression of *fnr* transcription by FNR is central to preventing a sustained increase in the steady state amount of total FNR under anaerobic conditions. The difference between the elevated level of *fnr* expression in the futile aerobic steady state and the level of expression needed for its physiological function in the anaerobic steady state represents an energetic cost to synthesize the extra mRNA and protein of the FNR system (~4100 molecules per cell under aerobic conditions versus ~2600 FNR molecules per cell under anaerobic conditions[14] at an average cost of 1225 ATP per FNR RNA and polypeptide synthesized[23]). Also the faster the over-expressed levels can be repressed during the dynamic transition from aerobic to anaerobic conditions, which is determined by the settling time, the lower the energy expenditure.

The repression of *fnr* transcription also facilitates a more rapid resolution to the anaerobic steady state. It has long been known in the engineering literature that enclosing a system within a negative feedback loop improves system robustness and response time, and that these properties can be quantified as long as the downstream processes are linear[24–26]. These general properties can be characterized quantitatively as well for biochemical systems embedded in a nonlinear context, provided the systems are carefully compared to an otherwise equivalent unregulated system as a control[27–29]. Although negative feedback plays a role in the temporal response FNR system, it is not a major contributor to the rapid initial response to transitions between aerobic and anaerobic conditions (see Supplemental Information). The interruption or reestablishment of an otherwise futile cycle is the major contributor.

The reintroduction of O_2 drives the restoration of the cycle and initiates a rapid depletion of active FNR (Fig. 3B). The model shows that this occurs because the environmental sensing

arm of the FNR cycle is driven by a faster reaction than the opposing arm in which active FNR is formed (Fig. 2). Under aerobic conditions, FNR is predominately in the inactive form, and ClpXP mediates the loss of inactive FNR. Because this process is significantly slower than O_2-dependent depletion of active FNR, the predicted time course for settling to the new *aerobic* steady state is again quite slow. The relaxation of negative feedback that coincides with the depletion of active FNR explains the modest increase in the total FNR pool, which causes the minor increase observed in the tail of the dynamic response in Fig. 3B.

The dynamics of shifting the cycle between its two states are analogous and involve a rapid initial transient caused either by interruption or restoration of the cycle, a distinct peak caused by feedback inhibition, and a protracted settling to a new steady state caused by slow loss of active FNR relative to the initial transient.

While the in vivo dynamics of FNR activation and inactivation have yet to be demonstrated directly, our model suggests an approach to capture the dynamics based on the temporal response of a reporter gene product. We discuss this approach below and show simulations that support the feasibility of this method. *β*-galactosidase activity in strains containing an FNR-dependent promoter such as *dms*A fused to the *lac*Z structural gene can be analyzed to provide insight into the dynamics of the shift to anoxic growth. By making frequent measurements of *β*-galactosidase activity during the aerobic-to-anaerobic transition, and analyzing the values and their derivatives in the resulting response curves, we can infer the *lac*Z transcription rate, which provides a bioassay of active FNR as a function of time during the transition (see Material and Methods). This process of inferring levels of active FNR by means of a reporter bioassay we term a *reporter inference assay*. Similar techniques have been used to assess the dynamics of other molecular systems[30,31]. We simulate this assay and show that it is capable of capturing the dynamic features of interest. This assay can also be done for the anaerobic-to-aerobic transition by starting in the anaerobic state and introducing O_2 at time zero.

The predicted dynamics for both active FNR and the reporter inference assay are shown for the aerobic-to-anaerobic transition in Fig. 3A and for the anaerobic-to-aerobic transition in Fig. 3B. This simulated assay predicts excellent agreement between the dynamics of active FNR and the inferred rate of reporter synthesis, which makes it a reasonable candidate for examining the *in vivo* dynamics of FNR in *E. coli*. The overshoot in the simulated reporter inference assay is approximately 20% larger than the final steady state of the reporter (dashed line Fig. 3A).

Optimum Cycling Rate

To understand the relationship between the rate of cycling and the regulatory role of the FNR circuit, we manipulated the cycling speed in the model and compared the dynamic responses for a series of altered systems. We examine this relationship by employing a mathematically controlled comparison[27,32] and predict experimental results for a FNR mutant intended to approximate the theoretical scenario. Our results show that the cycling rate of the FNR circuit under the conditions captured in our model is optimized for rapid switching between aerobic and anaerobic growth.

Mathematically controlled comparison—In order to appreciate how we conclude that the cycling rate of the FNR circuit can be optimized by selection to provide a rapid response, we first describe the central features of the controlled comparison. The method of mathematically controlled comparison allows us to alter the cycling speed of the model while controlling against unwanted changes elsewhere in the model. This is necessary because otherwise changing the rate at which FNR is transferred between the inactive and active forms (pools X_2 and X_3) would no doubt alter the steady state of the system. Changes in steady states of a nonlinear system can indirectly affect a variety of system attributes including robustness, capacity for regulation, local stability, and response times; such drastic differences would make the modified systems difficult to compare against the wild-type reference system. Using the method of mathematically controlled comparison minimizes the undesirable consequences of such changes by allowing us to equate the steady states of the modified and wild-type systems. In the end, we arrive at a more meaningful comparison. This is akin to requiring isogenic backgrounds for mutant strains in that one tends to eliminate extraneous differences, although the mathematics involved allows us to equate the mutant and the wild-type systems more rigorously. Further information on how this comparison is set up is available in the **Materials and Methods** section.

If the system is truly optimized for a rapid transition in response to changes in O_2 levels, and if cycling is central to this function, then an increase or decrease in cycling speed should produce a significant change in response time. The steady-state flux passing through the cycle in the wild-type system is given by $\alpha_{22}X_{30}X_{6,max} = 25.4\ \mu M\ min^{-1}$, where α_{22} is the rate constant for disassociation of dimeric FNR, X_{30} is the aerobic concentration of active FNR, and $X_{6,max}$ is the O_2 concentration in the aerobic state. The expression $\alpha_{22}X_3X_6$ represents flux through the left arm of the cycle in Fig. 2, whereas the corresponding expression $\beta_{22}X_2^2X_5$ represents flux through the right arm of the cycle. We define the cycling rate to be $\omega = \alpha_{22}X_{30}X_{6,max}$ ($\mu M\ min^{-1}$), which is the flux passing through the cycle in the aerobic steady state. The parameter α_{22} is the rate constant we will tune to change the cycling rate. In order to adjust the cycling rate (ω) in a mathematically controlled fashion without otherwise altering the state of system, we change the rate constants α_{22} and β_{22} in parallel (Fig. 2). We introduce a fold decrease/increase in α_{22} to achieve its new nominal value α_{22}'' (rate constant for disassociation of dimeric FNR) and calculate the corresponding value for β_{22}'' (dimerization rate constant) that balances the change in α_{22}'' (see Materials and Methods). Changing both arms of the cycle together is sufficient to select any cycling rate, while keeping the aerobic steady state of the system identical to the wild-type. Thus, before the transition from aerobic to anaerobic growth a family of FNR circuits with different cycling rates will all start in the same reference state. Their anaerobic states will all look different, and when transitioning from anaerobic to aerobic growth, the family of FNR circuits will all be transitioning to the same reference state. In this regard, we are comparing changes in the cycling rate of the FNR circuit relative to the aerobic reference state of the system. Since the system behaves primarily as a pathway under anaerobic conditions and a cycle under aerobic conditions, selecting the aerobic state as the reference is the logical choice.

The peak time, which captures the short-term response, is related to the cycling rate and hence the cost of cycling. The settling time, which captures the long-term response, also is related to cycling rate but the cost in this case is over-expression of mRNA and protein for the FNR system. Our analysis of the relationship between the cycling rate of the FNR model and its response time (peak and settling time) shows that there is a near optimum cycling rate (Fig. 4). As the rate of cycling (and hence energy expenditure) increases beyond this optimum (green areas in Fig. 4) there is little improvement in response time, but greatly increased energy dissipation that is clearly not optimal. On the other hand, as cycling rate decreases below this optimum (red area of Fig. 4), there is a trade-off between decreased energy expenditure and degradation in response time. Although the settling time does improve for the anaerobic-to-aerobic transition, this is more than offset by the marked slowing of the peak time. A rapid settling time for inactivation of FNR (dashed line Fig. 4B) comes at the expense of a marked delay in peak time (dashed line Fig. 4A); the potential 35% improvement in settling time corresponds to an 88% slower peak time. The optimization of the FNR model is perhaps best illustrated in panel C, where we sum the four response time curves (each curve is normalized against its maximum value). Clearly decreasing the cycling rate to save energy has a severe penalty in terms of the response time (red area of Fig. 4C), whereas increasing the cycling rate to speed the response yields only a marginal improvement at the cost of greatly increased energy consumption. Thus, the mathematically controlled comparison provides evidence in support of the hypothesis that selection can optimize the cycling rate of the FNR circuit for rapid switching between aerobic and anaerobic growth.

Proposed experimentally controlled comparison—The results of the mathematically controlled comparison are theoretical and do not lend themselves to simple experimental testing. While implementation of the experiments necessary to establish the optimal nature of the FNR cycling rate is beyond the scope of the work presented here, we would nonetheless like to suggest an approach for manipulating the FNR cycling rate in the laboratory and predict the outcome of such an experiment.

An experimental test that captures the central theme of our mathematically controlled comparison might be implemented with the use of two independent amino acid substitutions in FNR, one affecting each arm of the cycle. An example that reduces appropriately the dimerization of the monomer might be similar to the FNR-K152E variant in which a positively charged Lys is replaced by a negatively charged Glu at position 152 of the FNR protein[33]. The K152E variant lowers the flux through the right arm of the FNR cycle (Fig. 2) reducing the anaerobic steady state of active FNR to 70% of the wild-type value[33]. An example that reduces appropriately the inactivation of the dimer might be similar to, but less drastic than, the FNR-L28H variant in which a Leu residue is replaced by His in position 28 of the FNR protein[34]. The L28H variant lowers the flux through the left arm of the FNR cycle (Fig. 2) raising the aerobic steady state of active FNR to near that of anaerobic levels[34]. Creating this hypothetical double mutant may be difficult, since the examples mentioned above are not appropriately balanced in their effects, and experiments with these and other similar double mutants to date have not been successful in yielding functional protein (Kiley unpublished experimental results). Another complication might be effects that

these substitutions have on other functions of FNR. In any case, we can make predictions regarding the behavior expected of experimental comparisons with an idealized double-mutant.

By adjusting the values of α_{22} (rate constant for disassociation of the FNR dimer) and β_{22} (dimerization rate constant), we can mimic the behavior of each hypothetical mutant; by combining these mutant parameter values, we can predict the behavior of the hypothetical double mutant. This double mutant, if it can be constructed, should provide an experimentally viable analog of the mathematically controlled comparison by lowering the flux through both arms of the cycle in parallel.

The predicted dynamics of active FNR accumulation (Fig. 5A) and depletion (Fig. 5B) suggests that the hypothetical double mutant should lose the overshoot behavior and that the response time should be severely delayed for both activation and inactivation of FNR. In this example, the half-time required to activate FNR and bring about a transition to anaerobic growth is increased from the wild-type value of 0.1 minutes to 37 minutes. The half-time required to inactivate FNR and bring about a transition to aerobic growth is increased from the wild-type value of 0.02 minutes to 26 minutes. Active FNR is known to regulate hundreds of genes[12,13], which indicates that the slow switching times of the hypothetical double mutant could be expected to translate into significant misregulation and ultimately a slower growth rate relative to the wild-type when forced to transition frequently between the aerobic and anaerobic growth states.

Are the changes in response time of active FNR relevant to the environmental transitions *E. coli* experiences in nature? *E. coli* can be considered to have two major phenotypes, a ‘colon-type’ when in the lower intestine of warm-blooded animals and an ‘aquatic-type’ when in the external environment such as waterways and sewage treatment facilities[35]. These environments are each complex and poorly understood, but are clearly very different[21]. The organism’s normal life cycle is likely to consist of relatively long periods of slower growth in each anaerobic state punctuated by relatively brief periods of more rapid growth under aerobic conditions during transitions between these states[36]. For example, *transient strains* of *E. coli* enter the host, spend about 3 hours (as measured by the lactose tolerance test[37,38]) in rapid aerobic growth and a minimum of 24 hours (as measured by the transit time through the intestinal track[21,39,40]) in slower anaerobic growth, and then re-infect a subsequent host. Think of a diarrheal epidemic among infants in a newborn nursery. By contrast, *resident strains* enter the host, spend the same 3 hours in rapid aerobic growth, colonize the host’s distal small intestine and colon for anaerobic periods averaging several months (as measured by the recolonization rates in human volenteers[41–43], and then re-colonize another host. These are crude estimates based on clinical data (lactose tolerance test) and small samples with human volunteers (recolonization rates). However, this view of the *E. coli* life cycle is consistent with the molecular design of the well-characterized lactose operon[44]. Thus, the quicker *E. coli* can adjust to the anaerobic environment, presumably the more effective it can be in competing with the thousands of different types of resident microbes[45] during its colonization of the human gut.

Although it is clear that there is a trade-off between energy expenditure and response time and that the system seems poised at an optimum, we cannot be sure that response time itself is providing the selective pressure. It is always possible that some other process is responsible for the selection. Estimating energy costs and assessing their fitness effects is difficult. Thus a more direct examination of the natural transitions from aerobic to anaerobic conditions is needed, particularly for the very early events. For response times on the order of seconds to minutes to be important one would expect to see some experimental evidence of this in transitions from aerobic to anaerobic conditions. Rolfe et al[46], using transcriptional profiling with Bayesian approximation and a model involving a Markov process, have presented evidence suggesting transitions between aerobic and anaerobic conditions with response times on the order of 2 to 5 minutes. However, to demonstrate that these molecular changes can influence fitness, e,g, by changing the response time in growth of the integrated system, one would need a well-controlled experimental study to systematically change cycling rate and measure the corresponding changes in growth rate. As noted above, we have proposed such an experimental approach, although its implementation awaits construction of double mutants that meet the requirements for the experimental equivalent of a mathematically controlled comparison.

Conclusions

In contrast to truly futile cycles and to mechanisms in which the synthesis and degradation arms of a pseudo cycle are differentially regulated, the FNR system is unusual in that it takes advantage of a conditional futile cycle and as such represents a novel class of cyclic regulation. Our results argue that such systems represent a novel class of responsive signaling mechanisms capable of rapidly reprogramming gene expression. The main advantage in the case of FNR, and potentially other cyclic systems, appears to lie in having a fully prepared pool of effector proteins capable of directly sensing and acting on environmental stimuli.

Materials and Methods

Mathematically Controlled Comparison

The goal of a mathematically controlled comparison is to make a rigorous comparison of some specific characteristics shared by two systems, while ensuring to the extent possible equivalence between the two systems on all other characteristics[27,32]. We apply this approach to examine how changes in cycling rate affect the system response time. In the Supplemental Information, we also dissect different influences on response time using this approach.

Changing the Cycling Rate

The cycling rate ω is altered by selecting a value for $\alpha_{22}^{''}$ and solving for $\beta_{22}^{''}$ in the relationship $\alpha_{22}^{''}X_{30}X_{6,\max} - \beta_{22}^{''}X_{20}^{2}X_{5} = \alpha_{22}X_{30}X_{6,\max} - \beta_{22}X_{20}^{2}X_{5}$. The resulting value is given by

$$\beta''_{22}=\frac{\beta_{22}(\alpha''_{22}X_{6,\max}[K_2^n+X_{6,\max}^n]+\beta_{31,\min}K_2^n+\beta_{31,\max}K_{6,\max}^n)}{(\alpha_{22}X_{6,\max}[K_2^n+X_{6,\max}^n]+\beta_{31,\min}K_2^n+\beta_{31,\max}K_{6,\max}^n)} \quad (4)$$

For the purposes of comparison, we introduce a fold increase in the wild-type value of α_{22} (= 4.09 min^{-1} μM^{-1}) by integer increments from 2 to 100 and a fold decrease from 1/2 to 1/100. We assume aerobic and anaerobic growth rates that correspond to growth in glucose minimal media. This form of mathematical comparison allows for a change in cycling rate while maintaining the same steady state concentrations and throughput flux.

Reporter Inference Assay

To simulate the results of the reporter inference assay, we augment our model [Eqs (1)–(3)] by the addition of two equations.

$$dX_4/dt=\alpha_7X_3-\beta_7X_7 \quad (5)$$

$$dX_8/dt=\alpha_8X_7-\beta_8X_8 \quad (6)$$

Equation (5) describes the level of the *lac*Z mRNA under the control of a *dms*A promoter, which is induced by active FNR, and equation (6) describes the level of β-galactosidase protein. The rate constant for transcription, α_7 = 0.3 min^{-1}, is an estimate obtained by fitting the predicted steady state[18] of active FNR against previously published expression data[47] for a *dms*A-*lac*Z reporter construct. The rate of decay for the *lac*Z mRNA (β_7 = 0.48 min^{-1}) and the rate constant for translation (α_8 = 4.7 min^{-1} for the β-gal tetramer) were described by Kennell and Reizman[48]. We assume loss of the protein is a first order process that depends on exponential growth, since the β-galactosidase protein is stable and should only be diluted by cell growth (β_8 = 0.0077 min^{-1}).

Because of the stability of the β-galactosidase protein, turnover of the molecule is not rapid enough to clearly reveal the dynamic features of interest during an aerobic to anaerobic transition. However, the subtle changes in the rate of synthesis can be calculated from the observed activity using basic principles. If we rearrange equation (6) to highlight the rate of LacZ synthesis, we get the following.

$$\alpha_8X_7=dX_8/dt+\beta_8X_8 \quad (7)$$

The long half-life of β-galactosidase implies that the protein is accumulating much faster than it can be diluted by growth during the shift to anoxic conditions. Therefore, the measured β-galactosidase activity at a time *t* after the shift represents the integral or summation of effects from previous time points. A simple point-by-point derivative of the measured data provides the values for dX_8/dt in equation (7). By combining this information

with measured values for β_8 (growth rate) and X_8 (concentration of LacZ) one can calculate the rate of β-galactosidase synthesis, which in turn provides a bioassay for active FNR during the dynamics of the anoxic shift. The chief potential difficulty lies in the tendency of differentiation to exaggerate noise.

Supplementary Material

Refer to Web version on PubMed Central for supplementary material.

Acknowledgments

This work was supported in part by grants from the US Public Health Service (R01-GM30054 to MAS) and (R01-GM045844 to PJK). We thank Rick Fasani and Pedro Coelho for fruitful discussions on the FNR system.

Abbreviations used

apoFNR	apoprotein FNR
2Fe-FNR	$[2Fe\text{-}2S]^{2+}$ FNR
4Fe-FNR	$[4Fe\text{-}4S]^{2+}$ FNR

References

1. Bali M, Thomas SR. Comptes Rendus Académie Sci Sér III Sci Vie. 2001; 324:185–199.
2. Selkov EE, Avseenko NV, Kirsta YB. Biofizika. 1979; 24:829–835. [PubMed: 39635]
3. Hopfield JJ. Proc Natl Acad Sci U S A. 1974; 71:4135–4139. [PubMed: 4530290]
4. Ninio J. Biochimie. 1975; 57:587–595. [PubMed: 1182215]
5. Blanchard SC, Gonzalez RL, Kim HD, Chu S, Puglisi JD. Nat Struct Mol Biol. 2004; 11:1008–1014. [PubMed: 15448679]
6. Green J, Crack JC, Thomson AJ, LeBrun NE. Curr Opin Microbiol. 2009; 12:145–151. [PubMed: 19246238]
7. Lazazzera BA, Beinert H, Khoroshilova N, Kennedy MC, Kiley PJ. J Biol Chem. 1996; 271:2762–2768. [PubMed: 8576252]
8. Khoroshilova N, Popescu C, Münck E, Beinert H, Kiley PJ. Proc Natl Acad Sci U S A. 1997; 94:6087–6092. [PubMed: 9177174]
9. Mettert EL, Outten FW, Wanta B, Kiley PJ. J Mol Biol. 2008; 384:798–811. [PubMed: 18938178]
10. Lambden PR, Guest JR. J Gen Microbiol. 1976; 97:145–160. [PubMed: 796407]
11. Jones HM, Gunsalus RP. J Bacteriol. 1987; 169:3340–3349. [PubMed: 3298218]
12. Kang Y, Weber KD, Qiu Y, Kiley PJ, Blattner FR. J Bacteriol. 2005; 187:1135–1160. [PubMed: 15659690]
13. Salmon K, Hung S, Mekjian K, Baldi P, Hatfield GW, Gunsalus RP. J Biol Chem. 2003; 278:29837–29855. [PubMed: 12754220]
14. Sutton VR, Mettert EL, Beinert H, Kiley PJ. J Bacteriol. 2004; 186:8018–8025. [PubMed: 15547274]
15. Sutton VR, Stubna A, Patschkowski T, Münck E, Beinert H, Kiley PJ. Biochemistry (Mosc). 2004; 43:791–798.
16. Moore LJ, Kiley PJ. J Biol Chem. 2001; 276:45744–45750. [PubMed: 11581261]
17. Mettert EL, Kiley PJ. J Mol Biol. 2005; 354:220–232. [PubMed: 16243354]
18. Tolla DA, Savageau MA. J Mol Biol. 2010; 397:893–905. [PubMed: 20156450]
19. Tolla DA, Savageau MA. Mol Microbiol. 2011; 79:149–165. [PubMed: 21166900]

20. Boiteux A, Hess B. Philos Trans R Soc Lond B Biol Sci. 1981; 293:5–22. [PubMed: 6115423]
21. Savageau MA. Am Nat. 1983; 122:732–744.
22. Mettert EL, Kiley PJ. J Bacteriol. 2007; 189:3036–3043. [PubMed: 17293415]
23. Neidhardt, FC.; Ingraham, JL.; Schaechter, M. Physiology of the Bacterial Cell: A Molecular Approach. Sinauer Associates Inc; Sunderland, Mass: 1990.
24. Black HS. Electr Eng. 1934; 53:114–120.
25. Bode, HW. Network Analysis & Feedback Amplifier Design. Van Nostrand; Princeton, New Jersey: 1945.
26. Truxal, JG. Automatic feedback control system synthesis. McGraw-Hill; New York: 1912.
27. Savageau, MA. Biochemical Systems Analysis: A Study of Function and Design in Molecular Biology; 40th Anniversary Edition, CreateSpace; Charleston, SC. 2009; [A reprinting of the original edition, Addison-Wesley Publishing, Reading, MA, 1976.]
28. Savageau MA. Nature. 1975; 258:208–214. [PubMed: 1105191]
29. Hlavacek WS, Savageau MA. J Mol Biol. 1996; 255:121–139. [PubMed: 8568860]
30. Zaslaver A, Bren A, Ronen M, Itzkovitz S, Kikoin I, Shavit S, Liebermeister W, Surette MG, Alon U. Nat Methods. 2006; 3:623–628. [PubMed: 16862137]
31. Leveau JH, Lindow SE. J Bacteriol. 2001; 183:6752–6762. [PubMed: 11698362]
32. Savageau MA. Chaos. 2001; 11:142–159. [PubMed: 12779449]
33. Moore LJ, Mettert EL, Kiley PJ. J Biol Chem. 2006; 281:33268–33275. [PubMed: 16959764]
34. Bates DM, Popescu CV, Khoroshilova N, Vogt K, Beinert H, Münck E, Kiley PJ. J Biol Chem. 2000; 275:6234–6240. [PubMed: 10692418]
35. Savageau MA. Proc Natl Acad Sci. 1983; 80:1411–1415. [PubMed: 6219393]
36. Savageau MA. Genetics. 1998; 149:1665–1676. [PubMed: 9691027]
37. Bond JH, Levitt MD. Gastroenterology. 1976; 70:1058–1062. [PubMed: 1269865]
38. Malagelada JR, Robertson JS, Brown ML, Remington M, Duenes JA, Thomforde GM, Carryer PW. Gastroenterology. 1984; 87:1255–1263. [PubMed: 6092195]
39. Cummings JH, Wiggins HS. Gut. 1976; 17:219–223. [PubMed: 1269990]
40. Gear JS, Brodribb AJ, Ware A, Mann JI. Br J Nutr. 1981; 45:77–82. [PubMed: 6258626]
41. Sears HJ, Brownlee I, Uchiyama JK. J Bacteriol. 1950; 59:293–301. [PubMed: 15421958]
42. Sears HJ, Brownlee I. J Bacteriol. 1952; 63:47–57. [PubMed: 14927548]
43. Caugant DA, Levin BR, Selander RK. Genetics. 1981; 98:467–490. [PubMed: 7037535]
44. Savageau MA. Genetics. 1998; 149:1677–1691. [PubMed: 9691028]
45. Sears CL. Anaerobe. 2005; 11:247–251. [PubMed: 16701579]
46. Rolfe MD, Ocone A, Stapleton MR, Hall S, Trotter EW, Poole RK, Sanguinetti G, Green J, SysMO-SUMO Consortium. Open Biol. 2012; 2:120091. [PubMed: 22870390]
47. Tseng CP, Albrecht J, Gunsalus RP. J Bacteriol. 1996; 178:1094–1098. [PubMed: 8576043]
48. Kennell D, Riezman H. J Mol Biol. 1977; 114:1–21. [PubMed: 409848]

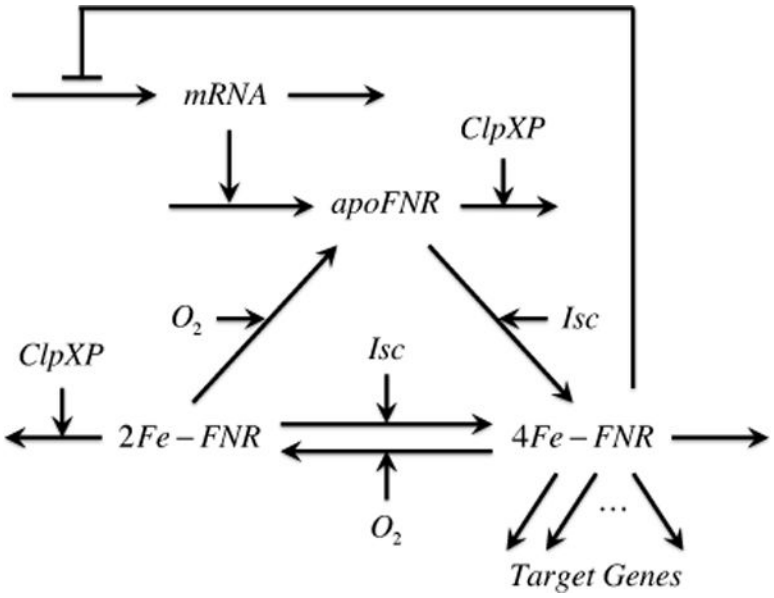

Figure 1. Representation of the FNR (fumarate nitrate reduction) System in *E. coli*

FNR regulates the shift between aerobic/anaerobic growth. Dimeric 4Fe-FNR adapts the cell to O_2 limiting conditions. Aerobically, O_2 inactivates FNR, but the cell continues to produce and reactivate it. This results in a constant cycling of FNR between its three states apoFNR, 4Fe-FNR, and 2Fe-FNR. Aerobic cycling is tuned so that the inactive apoFNR predominates. Under anaerobic conditions, the absence of O_2 results in a rapid buildup of 4Fe-FNR. The 4Fe-FNR form dimerizes to produce an active transcription factor controlling a large number of target genes.

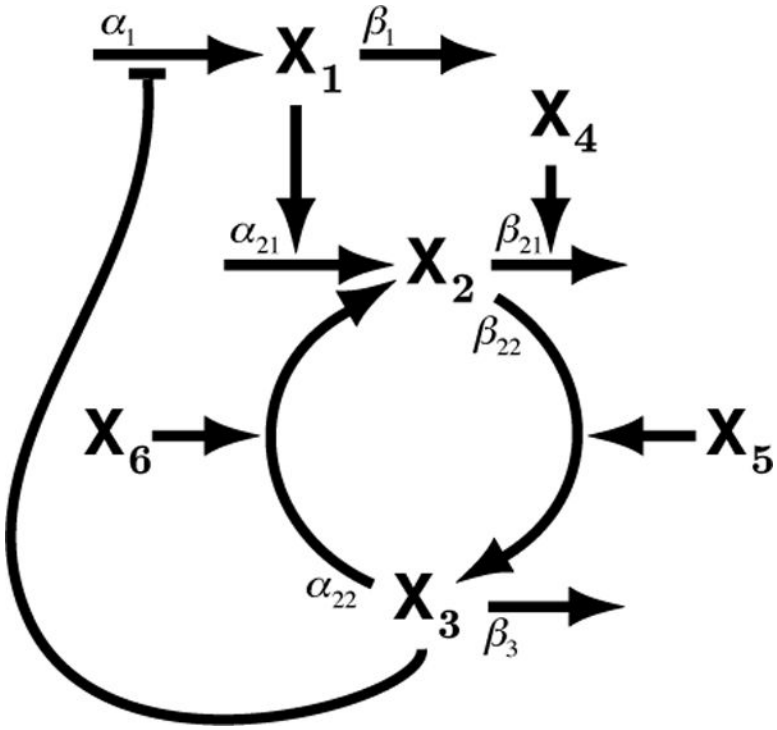

Figure 2. Diagram of the Kinetic Model for the FNR System

X_1 – *fnr* mRNA, X_2 – apoFNR and 2Fe-FNR, X_3 – 4Fe-FNR, X_4 – ClpXP protease, X_5 – iron sulfur cluster assembly proteins (Isc), X_6 – molecular O_2. The nucleotide and amino acid pools are assumed to be well regulated, and their nearly constant values are implicitly accounted for in the appropriate rate constants for transcription and translation. The fate of material lost from the system by degradation and/or dilution is not shown [See Tolla & Savageau[18] for further details]. The α and β symbols indicate the rate-constants for the corresponding rate-laws in the mathematical model given by Eqs. (1)–(3).

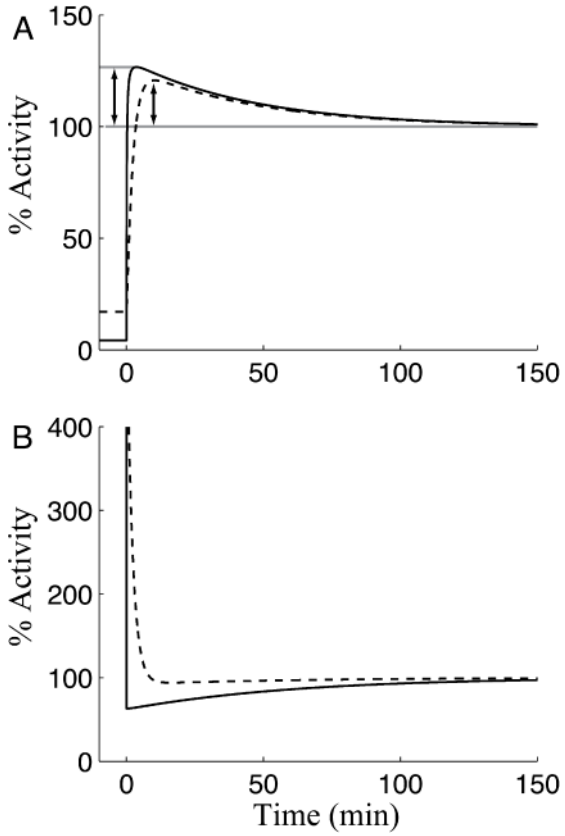

Figure 3. Dynamic Response of Active FNR to Changes in O_2

Predicted dynamics of active FNR (—) and its value inferred from the simulated *dms*A-*lac*Z reporter (– –). Each dynamic response is normalized with respect to its final steady state. (A) Predicted dynamics of FNR activation during the switch to anaerobic growth. The double arrows indicate the magnitude of the overshoot, which is 27% for active FNR and 20% for the *dms*A-*lac*Z reporter. (B) Predicted dynamics of FNR inactivation during the switch to aerobic growth.

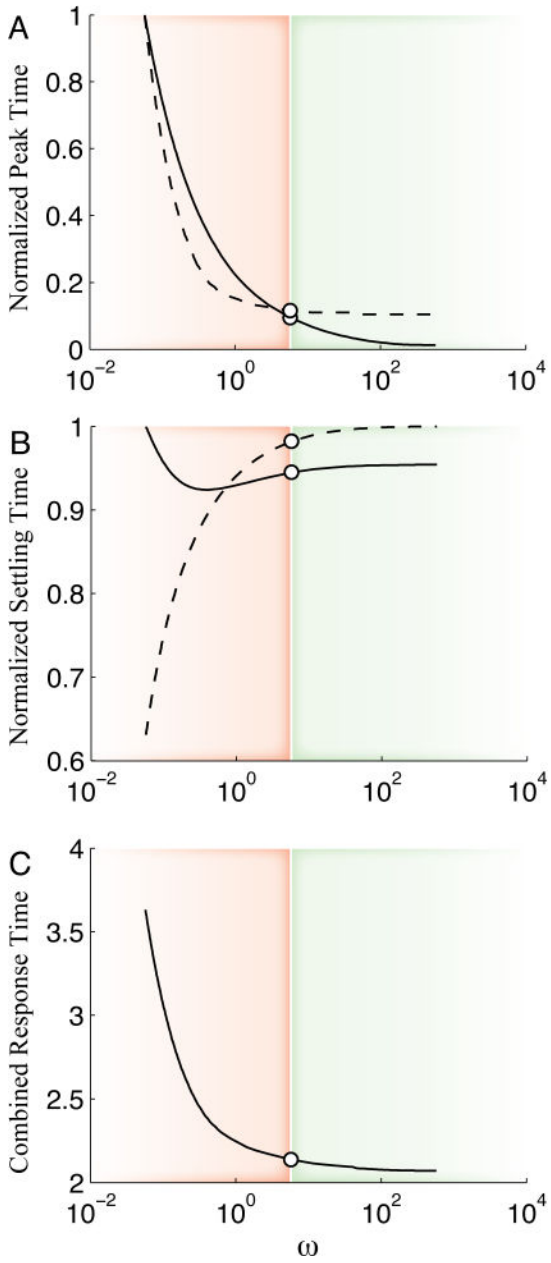

Figure 4. Predicted Optimum Cycling Rate

Relationship between cycling rate ω and the two temporal characteristics, peak and settling time, that characterize the dynamics of the FNR circuit. The open circle indicates the wild-type cycling rate. Red shading corresponds to a reduction in cycling rate and green shading corresponds to an increase in cycling rate. (A) Normalized peak time for the activation (—) and inactivation (– –) of FNR as a function of cycling rate. (B) Normalized settling time for the activation (—) and inactivation (– –) of FNR as a function of cycling rate. (C) Combination of all four normalized temporal characteristics as a function of cycling rate.

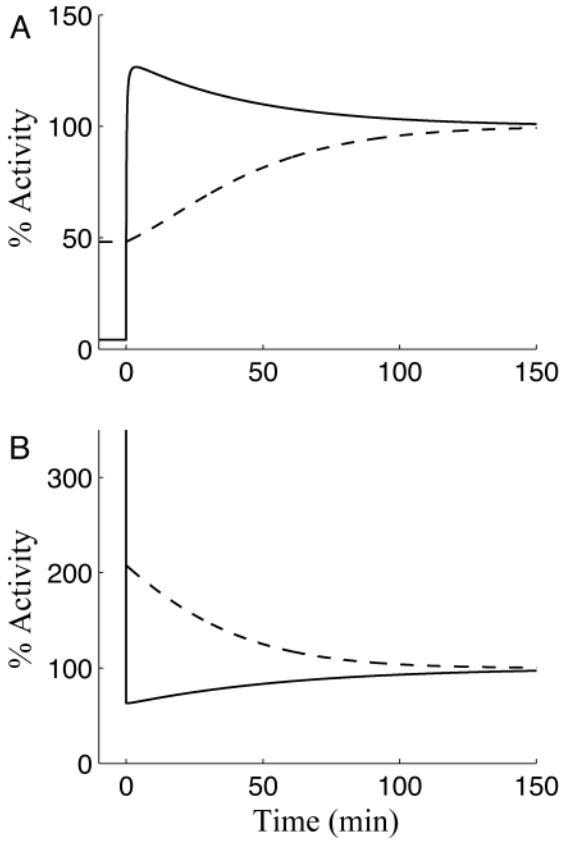

Figure 5. Simulated Temporal Responses that Show the Influence of Cycling Rate

Predicted dynamics of active FNR for wild-type (—) and the hypothetical double mutant (– –). (A) Predicted dynamics of FNR activation during the switch to anaerobic growth. (B) Predicted dynamics of FNR inactivation during the switch to aerobic growth.